PROJECT OF MINOR IN ENERGY

Spatial dispersion of photovoltaic panels in Switzerland and effect on electricity production

Sonia Dupuis

supervised by

Annelen KAHL CRYOS - EPFL

January 13, 2017

Contents

I. Acknowledgment

I would like to thank Annelen Kahl for her advice and guidance during all the semester for this project. Her availability throughout the semester has been of great help. Thank you also to Jérôme Dujardin for help with various technical issues. And finally thank you to the CRYOS LAB for accepting this semester project.

II. Nomenclature

The present section aims at giving an all inclusive list of the abbreviations used in this report.

List of abbreviations used	
Abbreviation	Full denomination
CI	Clear Sky Index
EUMETSAT	(European Organisation for the exploitation of Meteorological satellites)
MODIS	Moderate Resolution Imaging Spectroradiometer
masl or m.a.s.l	meter above sea level
NDSI	Normalized Difference Snow Index
PIS	Panel Icoming Shortwave
PV	Photovoltaics
SCD	Snow Cover Duration
SIS	Surface Incoming Shortwave
SLF	Institute for Snow and Avalanche Research
TIF	Tagged Image File

III. Introduction

Energy markets are currently facing a crucial change. In Switzerland, the Energy Strategy 2050[1] has been set up by the Federal Council. This strategy containing several measures should help Switzerland have a new energetic future. These measures should increase energy efficiency, increase the use of renewable energy and prepare a withdrawal from nuclear energy. In order to withdraw form nuclear energy and not be dependent on foreign electricity import, renewable energy production must be increased. Among all renewable energies that could be produced in Switzerland: hydraulic, wind, solar, geothermal -energies; the present report will investigate the potential of solar panel energy generation.

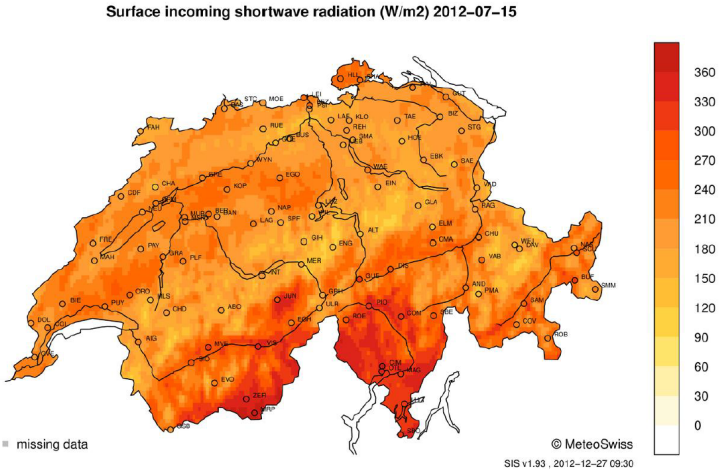

Figure 1: *Surface incoming Shortwave [W/m^2], MeteoSwiss*

The figure above represents the surface incoming shortwave (SIS) radiations for a summer day in Switzerland. This country presents potential for using solar energy, especially in some regions (Wallis and Ticino, for example) that receive more radiations. These regions presenting high mountains profit of less scattering of radiations at these altitudes (Barlett et al.). The slope and orientation of the terrain is also important, this way a south-facing slope receives more solar insolation than another oriented slope. In Barlett et al. the difference of power generation across seasons is exposed, as well as an asset of Switzerland being renewable. There is a mismatch between demand and offer of energy during winter.Therefore, the effect of snow cover on sun ground reflection will be investigated. The high albedo of snow increases the ground reflection component of the panel incoming shortwaves (PIS). The winter energy production could thus be

[1] http://www.bfe.admin.ch/energiestrategie2050/index.html?lang=en

increased. The albedo data is computed from MODIS data. This instrument on NASA's satellite provides multispectral images of the earth. MODIS snow products are used widely for asserting snow cover. For example in the study of He et al. 2014.

IV. Research Questions

The scope of this project is to study if the snow cover affects the ground reflectance of Surface Incoming shortwave Radiation (SIS) and influences PV electricity production, particularly winter production. The idea is to decrease seasonal mismatch by increasing winter production thanks to snow cover. In a second step, the best location for PV panels in terms of snow duration will be sought. In order to explore both extreme of the influence of snow cover reflectance on production, two scenarios for implementing PV panel will be investigated:

- The first: based on location of high snow duration.
- The second: based on the assumption that PV panels are installed on rooftops in cities, is linked with population density.

V. Data

The data used for this project are:

- Satellite based radiance for Switzerland made available form MeteoSwiss and provided by A.Kahl. The radiance was monitored with METEOSAT, a geostationary satellite from EUMETSAT (European Organisation for the exploitation of Meteorological satellites) recording Earth landscape images and meteorological data. Previous studies at the Cryos lab (EPFL) were done with these data (Bartlett et al. 2015); The data sets are structured in grid form, the grid covers entire Switzerland and has a size of 103x241 pixels. These data are computed by a complicated algorithm and a method for distinguishing a cloudy day from a clear sky day. These computational steps and theoretic explanations are presented in the scientific report*"The Heliomont surface solar Radiation processing"* explaining the provenance of SIS (Surface incoming solar) radiation, published in 2013 by MeteoSwiss.

  Data covers the time period form January 2009 to December 2014. The data is stored in Matlab-readable matrices :

  - SolarAngles365_hrly_UTC_0430am_1030pm_UTCplus1.mat *computed by solarangle.m*
  - SIS_MetaData_from2009.mat

  - SIS_Data_hrly_from2009.mat
  - SIS_beamparallel_Erbs_from2009.mat *computed by Transform_SISbeam2BeamParallel.m*
  - Referencing_Matrix.mat
  - Ratio_diff2global_hrly_OH_from2009.mat *computed by Compute_Ratio_Diffuse2Global.m*
  - Ratio_diff2global_hrly_Erbs_from2009.mat *computed by Compute_Ratio_Diffuse2Global.m*
  - Ratio_diff.mat

- Clear sky index (CI) data. One of the main challenge with computing SIS data is the detection of clouds. In order to make the difference between a clear-sky day and a cloudy day, a clear sky index has been introduced. The cloud index used here *" relies on the accurate retrieval of the clear sky reflectance as a reference for cloud free situations"*[2] (Stöckli 2013). The Data for clear sky index is in grid form (103x241 pixels):
  - CI_MetaData_from2009.mat
  - CI_Data_hrly_from2009.mat

- Corine Land use cover of Switzerland. It represents the country by inventorying land cover in several classes (32, here).[3] The list of the corine classes and associated descriptions are showed in Appendix I.
  - CLC_CH_2012.shp

- Elevation grid for Switzerland.The grid has the same size (103x241) as the radiance grid.
  - DEM_matched.mat

- Masks for Switzerland (Mask_all.mat, size 103x241). Masking out the lakes, and altitude above 2'500 m.a.s.l.
  - Mask_AltiSup2500.mat
  - Mask_Country.mat
  - Mask_Lakes.mat

- Matrix (103x241) with population density for each pixel: pop_norm.mat

[2]Reto Stoeckli: 2013, The HelioMont Surface Solar Radiation Processing, Scientific Report MeteoSwiss, 93, 12 p.
[3] http://www.wsl.ch/fe/landschaftsdynamik/projekte/corine_landcover_update/index_EN

- Data for feasible area per pixel for installing PV panels (feasible_area.mat). The matrix is obtained with the Matlab-code "Find_Fesible_Area_AK.m" from A.Kahl and Viet Anh. The table below lists the fractional usable area per pixel.

Fractional cover for each landcover type	
Landcover type	Fractional cover
Urban	0.1
Industrial, commercial and transport units	0.1
Mine, constructions	0
Artificial non agricultural vegetated areas	0.05
Arable land,	0.05
Permanents crops	0.05
Pastures	0.08
Heterogeneous agricultural areas	0.08
Forests	0.05
Shrub/herbaceous	0.08
Open space with little or no vegetation	0.1
Inland wetlands	0
Inland water	0

- MODIS (Moderate Resolution Imaging Spectroradiometer) NDSI snow cover and Albedo data from *Aqua* satellite, with 500 m spatial resolution and daily time resolution from January 2009 to December 2013. The NDSI and Albedo values are given in a range from 0 to 100 as described in the *MODIS Snow Products Collection 6 User Guide* (A. Riggs, K.Hall, and Roman 2016) . The NDSI is calculated by a reflectance ratio of band 4 and band 6 of MODIS. (Salomonson and Appel 2004)

$$NDSI = \frac{band4 - band6}{band4 + band6}$$

A set of Matlab-codes have been used in every step of this project, the complete list of them with a short description is to be seen in the Appendix. The main operations that these codes fulfil are explained in this section. In order to obtain the final shortwaves that reach the PV panels (PIS) from SIS and CI data, there are several steps.

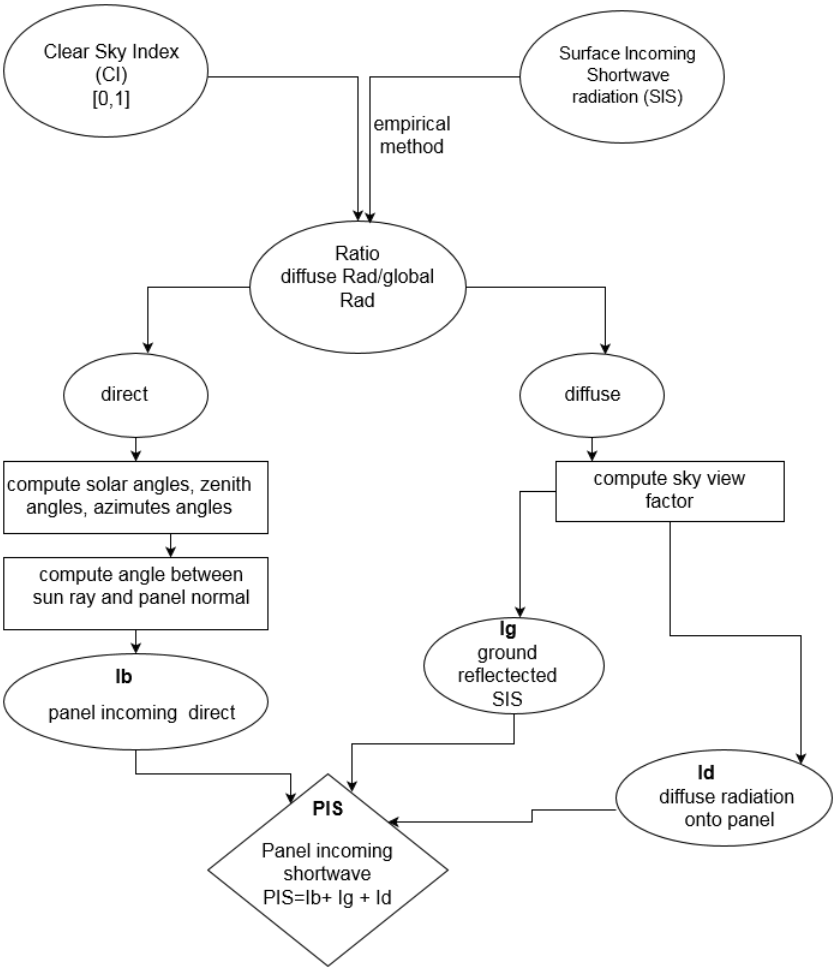

Figure 2: *Schema for obtaining PIS, provided by A.Kahl*

The first step consist in computing the ratio of diffuse radiation. There are two methods: Erbs and Orgill Holland (Duffie and Beckman, 2013). Both methods are executed in the code and compared. The relation used later on in the project is that form Erbs. Then, the solar angles (zenith and azimuth) for each SIS pixels are computed. The components of PIS (I beam, I ground and I diffuse) are computed afterwards. The I diffuse component is a function of the SIS Data, the diffusion ratio and the angle of the tilt. The I ground component is calculated by multiplying the SIS Data by the reflectance value of the ground and projecting this with the tilt angle. The I beam component is a function of the solar azimuth and zenith angles, and the beam parallel radiation (previously computed). The PIS computations are done for various tilt angles (15°, 30 °, 34°, 45°and 60°) and azimuths (SE, SSE, S, SSW, SW), therefore for the computation of the components the projection factors for each different setting are taken into account.

Matlab codes are also used for treating MODIS and Corine Data, as well as for computing and comparing the two end scenarios.

VI. Methodology

I. SIS Computation

The codes provided by A.Kahl compute from the clear sky index and the surface incoming shortwave radiation, the final panel incoming shortwave. This value is the final value quantifying the amount of radiation reaching the panel. The data in organised in grids of 103 x 241 pixels covering all of Switzerland. The spatial resolution is 1.6 km x 2.3 km, approximately because being converted from arc seconds at Swiss latitude and longitude. The temporal resolution is hourly. SIS Data is obtained only for hours getting sunlight, meaning more hours in the summer months and less in the winter months. In order to calculate the ground reflected component (Ig) the SIS data is multiplied by a reflectance factor and a tilt angle factor. The reflectance is highly variable, even more during the winter season when snow covers a wide area. This reflectance factor is computed by a combination of albedo values obtained from MODIS products and a reflectance assigned to a given class defined by the Corine map of land use. Albedo values are used when snow is present. If there is no albedo value (detected by the satellite as having no snow on the pixel) on a pixel, the Corine reflectance value is assigned.

II. MODIS Data

II.1 MODIS Instrument

The MODIS sensor is an embeded instrument on the Terra and Aqua satellites. This instrument provides multipsectral images distributed in 36 spectral bands from 0.4 μm to 14.4 μm.(*MODIS Web* 2016). A double-sided mirror is used in order to optimally record images for the whole spectral range above land, ocean and atmospheric medium. The spatial resolution of the MODIS product is 500 m. The high accuracy, especially when the sky is clear, and availability (every day) make the MODIS data valuable for snow cover monitoring as stated by Klein and Stroeve 2002. The main key drawback using MODIS data is the presence of cloud (Tang et al. 2014).
For the purpose of this project the MODIS product MYD10A1 has be chosen for his snow data (A. Riggs, K.Hall, and Roman 2016). The MODIS images are presented in a tile form. They have been downloaded from the reverb site from the NASA: *https://reverb.echo.nasa.gov/reverb*. On this

web site, for downloading the desired data the boundaries of the tile are entered by a box or by coordinates, the desired dates and the product are chosen.

The tiles are covering Switzerland and are available at a daily frequency. Among the images downloaded a NDSI snow cover and a Snow Albedo tile for each day have been downloaded. The tiles are downloaded for a period from the 1st of January 2009 to the 31th of December 2013.

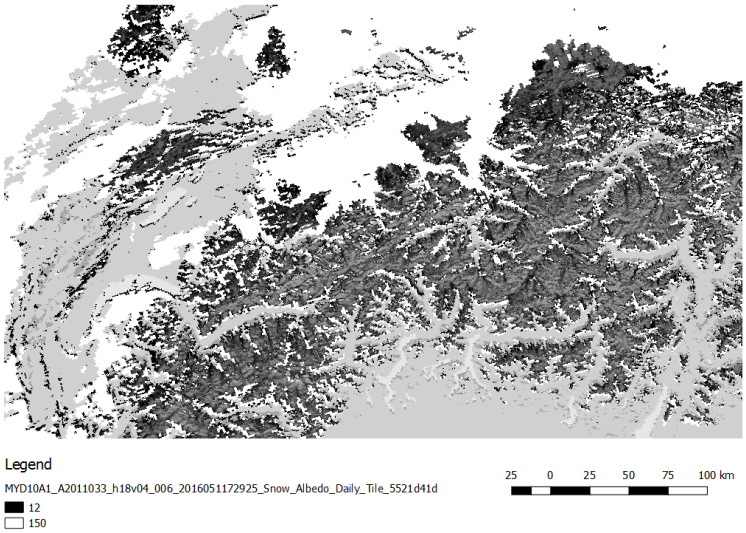

Figure 3: *Albedo*

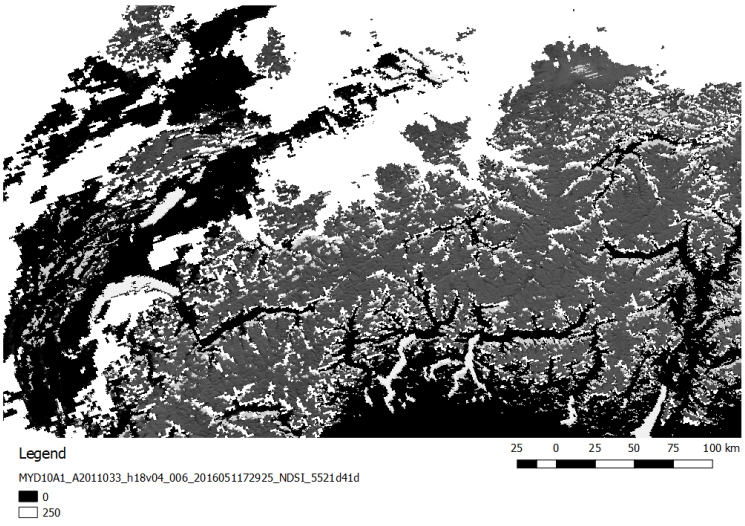

Figure 4: *NDSI*

II.2 MODIS - Data treatment

The previous tiles, to be used in the project have to be converted into a SIS-grid format, meaning having 103x241 pixels and matching this SIS grid.This will allow to assign to each SIS value a reflectance value. This conversion has been done with help of QGIS and MATLAB. First, the SIS_PixelArea.tif and one of the MODIS tile are imported to QGIS. The projections of both grids have to be chosen carefully. Both are assigned to a WGS 84 projection. Then, a grid is made on both TIF images. This is done with the griding tool, under Vector/Research Tools/Vector grid. in "Grid extent" the TIF is chosen and in "grid type" *output grid as polygon* is selected. This is done for both grids. Then, the grids have to be saved under the LV03 projection. An intersection is made from both grids. The MODIS grid is intersected with the SIS grid by help of the intersection tool under Vector/Geoprocessing Tools/Intersection. The output represents a new shapefile with all the intersections represented as little polygons. The surfaces of the polygons are calculated with the field calculator in the attribute table in QGIS ($area). From the attribute table of this shapefile, the ID columns of both grids as well as the surfaces are exported in a CSV-file. The columns in the file are ranged this way: 1) ID of MODIS pixel (small pixels), 2) surface of SIS pixels, 3) ID of SIS pixels, 4) surface of MODIS pixels. This file is then treated in Matlab with the "MODIStoSIS" code. the code computes then the mean of the MODIS pixel values contributing to one SIS pixel.

II.3 Interpolation

As described in the Userguide of the MODIS products, many values correspond to cloud cover or cannot be used. These values are interpolated through time, with a linear interpolation. This is done with the "interpolation" code. At the end we have an albedo and a NDSI value for every day. It is to be noted, that the albedo corresponds to full pixel albedo, and is not necessarily the true snow albedo. For the purpose of this report, the full pixel albedo is used.

III. Corine Land Use

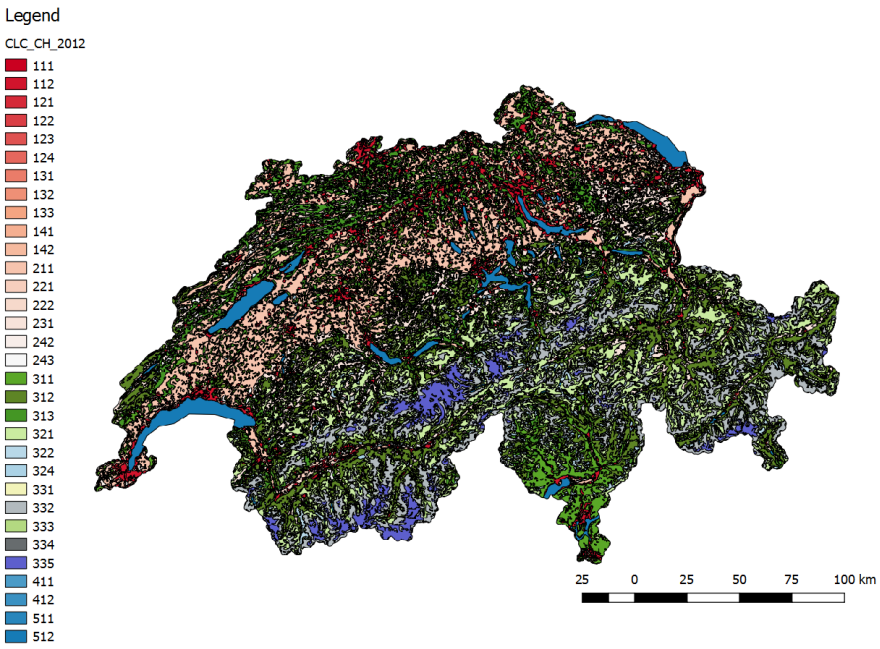

Figure 5: *Corin map*

This map represents Switzerland divided into classes of land use and activities. The legend of the map is in Annexe I. The Corine vectorial shapefile is rasterized with Arcgis and then treated in Matlab to correspond to the SIS grid. For every class a reflectance has been assigned, following the table below. the reflectivity values for the surfaces come from Oke, 1992 and Ahrens, 2006.

Reflectance of Corine classes	
Classes	Reflectance
111, 112, 121, 124 (artificial surfaces)	0.18
141, 142 (artificial, non-agricultural vegetated areas)	0.2
211, 221, 231 242, 243 (agricultural areas)	0.2
222 (fruit trees and berry plantations)	0.17
311, 312, 313 (forests and semi-natural areas)	0.1
321 (natural grasslands)	0.16
332 (bare rocks)	0.35
333 (sparsely vegetated areas)	0.1
411 (inland marshes)	0.1

The few remaining classes are assigned to 0.2. It is to be noted that the classes corresponding to lakes and water bodies as well as those at too high altitude are masked out in the project. therefore, they are not taken into account, here.

IV. Reflectance Computation

As a result, the reflectance values acquired from the MODIS data and the Corine map are aggregated in a daily reflectance map. The Corine-reflectance values are constant through time. This map is then masked with the lake-, altitude- and country mask, keeping only the relevant pixels for the study. These remaining pixels containing the daily reflectance values then replicated for each hour of SIS data corresponding to each irradiance day, i.e the irradiance duration for one day is not constant, in winter there are less hours for one day than in Summer.

V. Panel Component Computation

The various components of PIS (Ig, Ib and Id) are computed with the code: Radiation_onTiltedPanel_loop. The resultant value is a matrix Ipanel (9742x4776x25). There are three dimensions: the first represents the useful pixels, the second the hours for one year and the last one, the tilts and orientations of the PV panels. Four Ipanel matrices, one for each year from 2009 to 2013 are computed.

VI. Snow Cover

The albedo tiles from MODIS were used to compute the reflectance, the NDSI tiles, are here used for calculating the average snow duration for each pixel. The threshold chosen for saying that a pixel is covered with snow is a fractional snow cover of 60%. The number of snow days is then counted for each pixel.

VII. Scenarios

With the data obtained before, two scenarios for installing PV panels have been imagined. The goal was to investigate the effect of snow cover on electricity production. To do this, two extremes scenarios have been chosen: one scenario based on the presence of snow and another, an urban scenario based on the population density. It is assumed that for the most populated cities(Zürich, Geneva, Lausanne, Basel and Bern) snow is almost never present. For both scenarios, the target production has been fixed to 12 TWh. This target production is an assumption for the contribution of the solar energy production to the total 20 TWh that have to be produced with renewable energies in order to replace the nuclear energy. In both scenario, the aspect and the slope of the

PV have been fixed, in the best productive settings for the snow scenario. An additional scenario, with an optimal tilt angle for the urban scenario has been computed. This was done to verify that the difference observed between both scenarios was not only due to the difference in tilt angles. Panels are south facing and having a tilt angle of 60°. The efficiency of PV for domestic use, commercialised in Switzerland is assumed to be 15 %. [4]

VII.1 Snow Scenario

The PIS values, stored in the Ipanel matrices, for each pixel are multiplied by the PV efficiency and by the feasible area for each pixel. The feasible area for each pixel is computed with the code : find feasible area. This code computes the available area for installing PV panels per pixel with the corine map. To each major class is assigned a feasible percentage for installing panels. For this scenario the winter period goes from 1st of January til the end of April. The pixels are then ranked from the most productive to the less ones. The number of pixels, and thus the area needed to reach the target production is then computed. The surplus production due to the pixel unity is deduced from the total area.

VII.2 Urban Scenario

In this scenario, the PV panels are assumed to be put on rooftops of big cities. The electricity demand is the highest in big cities with a high population density. Therefore, putting the PV panels there will locate the production near to demand. To choose the pixels located in the cities, the pixels are ranked by their population density, with help of the matrix "pop_norm". The pixels having the greatest population density are at the top. To get the final area needed for reaching the target production, the PIS values are multiplied, as before, by the feasible area. The surplus production is also deduced in the end.

VII. Results

I. Analysis of PIS components

The figure below presents the different components for the PIS, as well as the SIS data. Panel-incoming direct represents the Ibeam component, ground reflected : the Iground component and the allsky diffuse represents the Idiffuse component. The pixel picked here for display is situated in Wallis, in the mountains at 2'493 masl. The precise localisation is displayed in the Appendix

[4] www.energyscope.ch

(fig. 16). We can can see that the ground reflection is at its highest during the first trimester of the year, corresponding to the winter season. In the Appendix are shown the same display with the same pixel for a different orientation and tilt angle (fig.17 and 18). 60°is ideal for ground reflection enhanced with snow cover.

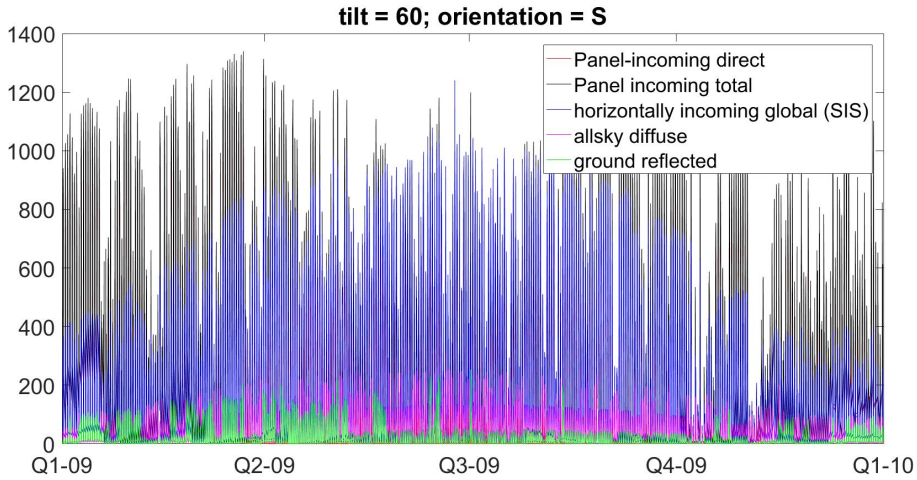

Figure 6: *Behaviour of PIS components with a tilt angle of 60°and a south orientation*

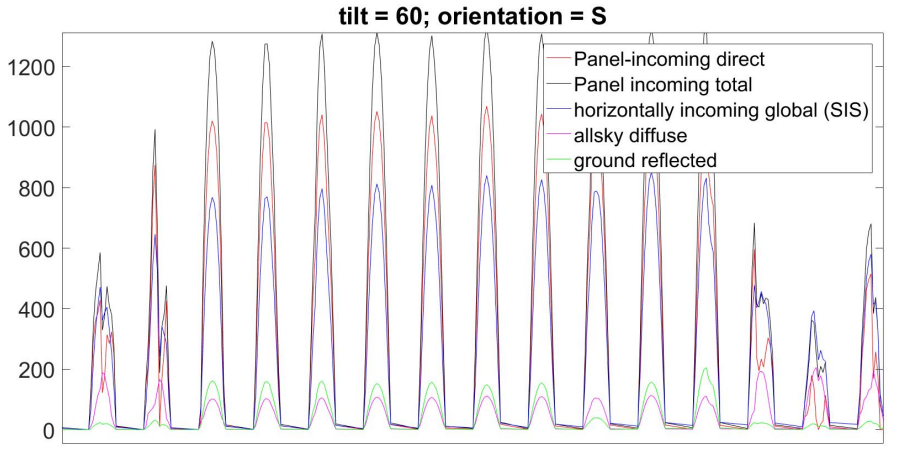

Figure 7: *Zoom on daily scale, each peak represents one day*

In the figure above, the same representation has been zoomed in. In the middle of the picture, we can observe sunny days, having a high peak of panel incoming shortwaves. On the right of the pictures, cloudy days with less incoming radiation can be observed. By cloudy days, there is more

diffusion, so the allsky diffuse component is higher than during sunny days, and is at the same level than the other components.

II. Snow Duration

The plot below shows the mean annual snow duration as a function of elevation for the year 2013.

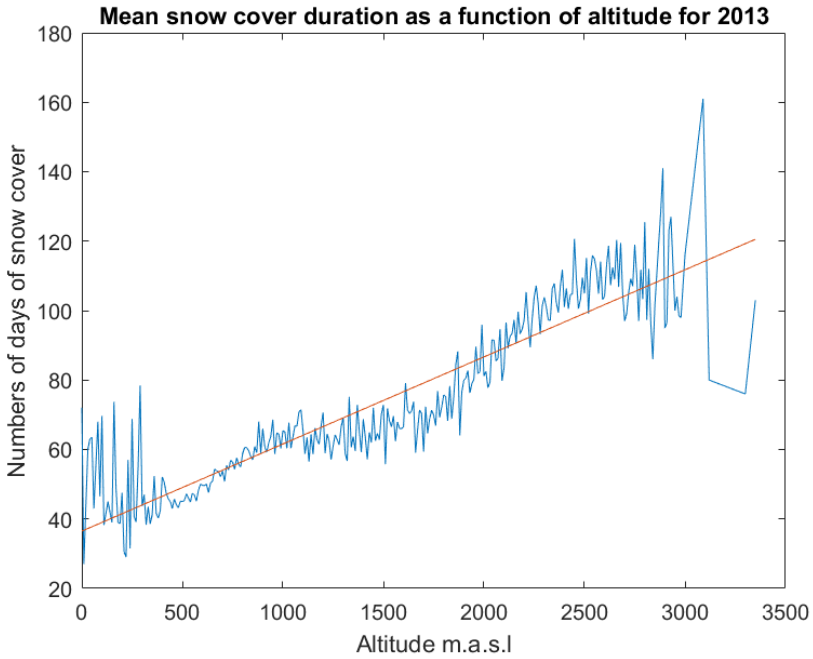

Figure 8: *2013*

The results for the previous years (2009, 2010, 2011 and 2012) are showed in the Appendix (fig.19 to fig.22). The table below summarizes the intercept and slope coefficients of the linear fit and gives information about the snow cover duration (SDC) in number of days from the linear fit at elevations 1'000 masl and 2'000 masl.

Linear fitting coefficients				
Year	Intercept	Slope	SCD at 1000 masl [days]	SDC at 2000 masl [days]
2009	38.6240	0.0251	63	89
2010	34.573	0.0247	59	84
2011	19.4320	0.0298	49	79
2012	31.1832	0.0228	54	77
2013	36.5005	0.0251	62	87

In figure 8 we can see that the values under 500 m.a.s.l are highly variable, this is due to various reasons. Satellite data that are not really accurate in regions near lakes and inland waters and high meteorological variability and instabilities at low values could be an explanation. The tendency for all the years is the approximately the same and shows a correlation between altitude and snow cover duration. The maximum of snow cover days is between 160 and 180 for all examined years.

In the study of Hüsler et al. 2014, the variations of snow cover durations for five geographic regions are investigated. The figure below[5],*"displays the SCD as a function of altitude and was calculated from all the pixel information available per 100m altitude in the respective region."* A positive correlation between altitude and SCD can be seen. They observed that at low elevations the differences between regions in SCD are greater. SCD at low altitude could be more sensitive to temperature variations than at higher altitudes. The temperatures neber being below zero for an extended period.*"The amount of snow present in the Alps varies considerably over the course of one year. The seasonal snow cover generally starts to increase in November, reaches a maximum between January and February and starts to melt out in mid-March. By the end of May, almost all snow has disappeared except for the very high areas lying above 2500 ma.s.l."*

[5]figure 6,p.82 in their article

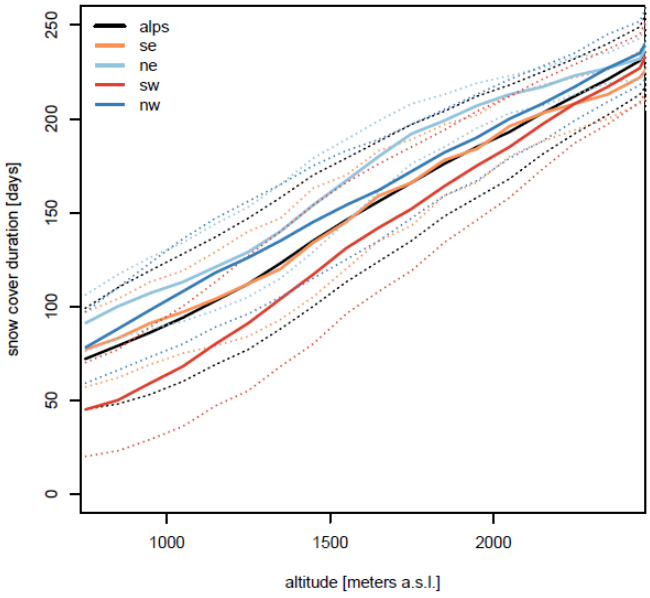

Figure 9: *Snow cover duration [days] as a function of altitude [m.a.s.l]. Bold lines represent the altitude mean SCD and the dotted lines indicate the standard deviation. From Hüsler et.al*

The difference shown between the graph of Hüsler and the one on figure 8 could be due to the pixel size and the satellite derived data quality. The other element that may influence SCD is the snow percentage threshold chosen for saying that a pixel has snow on it (60% in this project).

III. Snow Scenario

The table below summarizes the needed area for installing PV panels with the snow scenario for different years.

Area needed	
Year	Area [km^2]
2009	48.36
2010	44.87
2011	44.12
2013	41.39

The needed area is decreasing towards present. The variations could be explained by different meteorological conditions: changing snow cover and snow duration as well as sun insolation. The

localisation for PV panels are shown in the figure below. The detailed figures for all years are shown in the Appendix (fig. 23 to fig. 26).

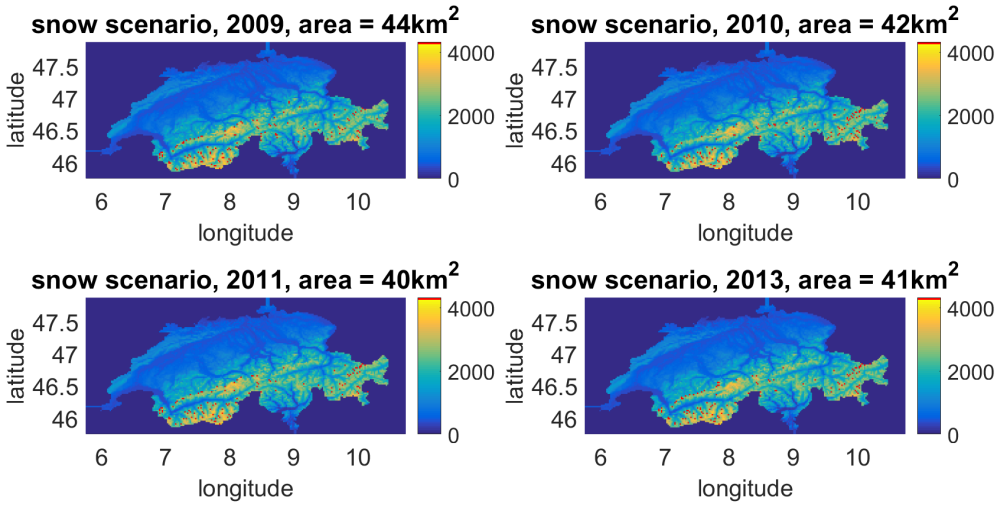

Figure 10: *Snow Scenario*

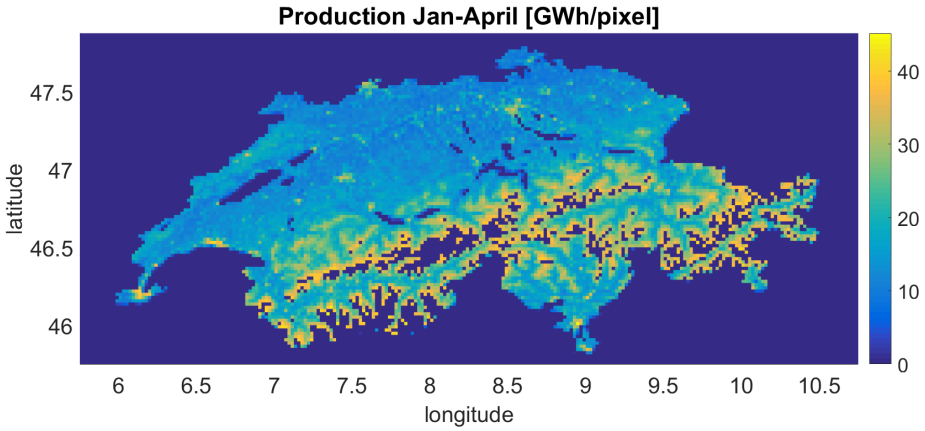

Figure 11: *Production Januray to April*

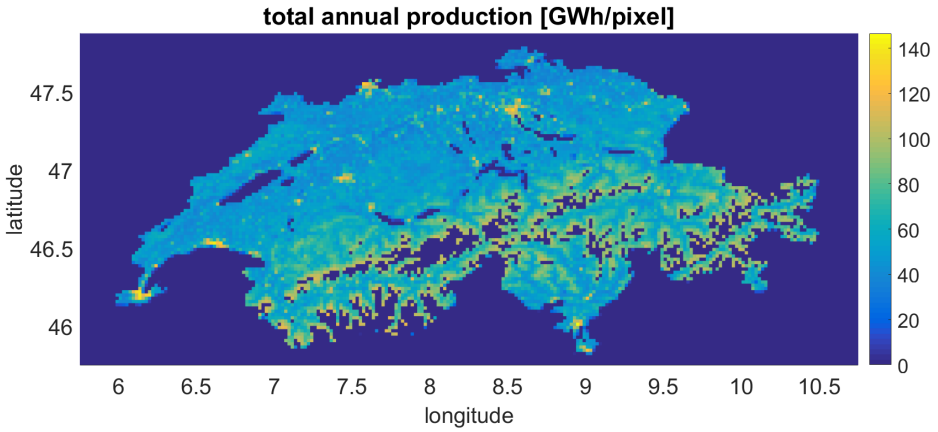

Figure 12: *Total Annual production*

The figure above show the exclusive winter production and the total annual production for all pixel in Switzerland under 2'500m. The hourly production of the snow scenario has been passed into the power flow model of J.Dujardin and A.Kahl. Their work "Impact of combined photovoltaic and wind energy on a fully renewable Switzerland" presents the possible combination of renewable energies for power generation. Import and export of electricity are necessary for compensating power demand mismatch even if the design of the installation is optimal (Dujardin et al, 2016). Storage corresponds to the dams reservoirs, which are filled up when the price of electricity is low. These are the results obtained:
Forced export: 894 GWh
Required short-term storage with forced discharge: 29.07 GWh (without forced discharge: 60.5 GWh)
Storage losses: 394 GWh
Total annual import with forced discharge: 4456 GWh, (without forced discharge: 4207 GWh)

IV. Urban Scenario

The table below summarizes the needed area for installing PV panels with the snow scenario for different years. The precise images are displayed in the Appendix (fig. 27 to fig. 30).

Area needed	
Year	Area [km^2]
2009	56.59
2010	59.29
2011	51.50
2013	59.73

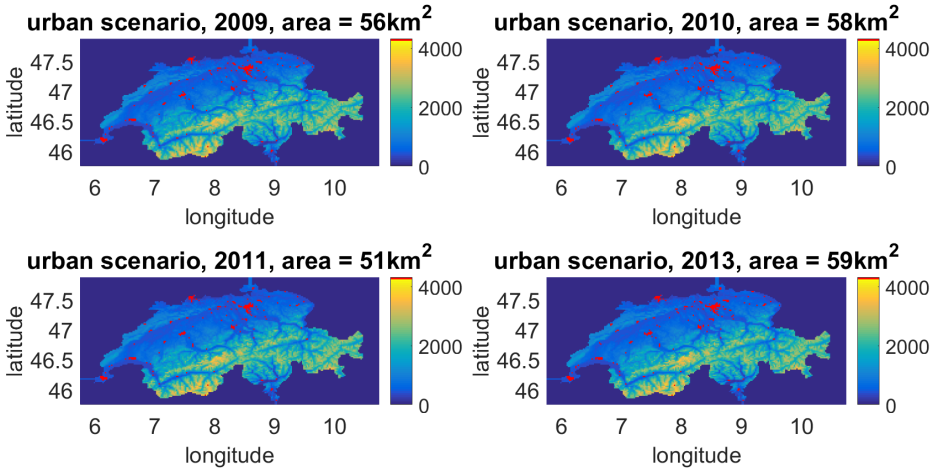

Figure 13: *Localisation of PV panels*

The figure above describes the localisation of the PV panels for the urban (population density) scenario. As the ranking does not change across years, the location of PV panels is the same, only some panels are added if more area is needed. As desired by the scenario, the PV panels are concentrated in big cities. This shows that installing PV panels only on rooftops in the cities is possible for generating the target production

The data has also been put in the same power flow model, here are the results:

Forced export: 1478 GWh

Required short-term storage with forced discharge: 31.8 GWh, (without forced discharge 83.4 GWh)

Storage losses: 586 GWh

Total annual import with forced discharge: 5854 GWh, (without forced discharge: 5640 GWh)

The figure below shows the comparison between both scenarios. A variation with the urban scenario has been made. The urban scenario was run once with the tilt angle at 60°and another time at the urban best tilt angle.

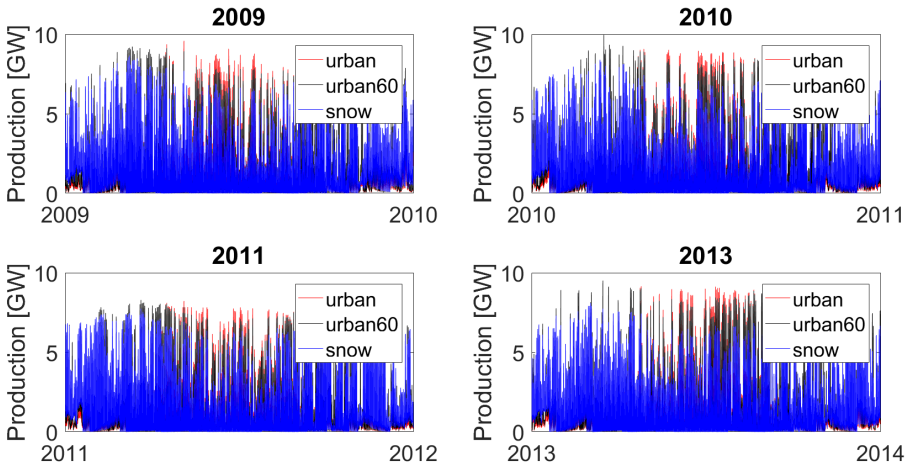

Figure 14: *Comparison of scenarios*

VIII. Discussion

More area is needed for the urban scenario, this is due to the fact that the snow reflectance improves the winter production and that the PV panels located on pixels with long snow duration are located in area where the solar radiance is globally higher, for example places in Wallis and Ticino. .

The following figure quantifies the difference in production between the snow scenario and the urban scenario.

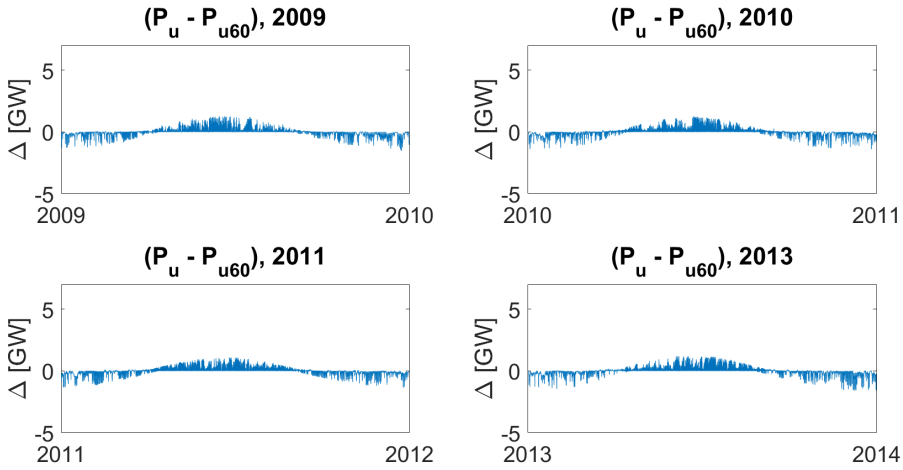

Figure 15: *Comparison of snow scenario and urban scenario with 60° tilt angle*

It is interesting to see that the snow scenario produces more in winter due to the presence of snow and greater ground reflection, during the summer months the urban scenario is more productive, the tilt angle chosen for snow being highly productive only if the ground reflectance is high. The import is also lower with the snow scenario, due to more production in the periods when demand is high. The forced export is lower too. Using snow reflectance helps matching the power offer closer to the demand and generating less import/export.

IX. Conclusion

This project was really interesting and challenging. It was dealing with an actual problematic and concrete solutions to solve it.

It shows that it is possible to install renewable settings in Switzerland and that the potential is high. Both scenarios tested here could be considered. It demonstrates that snow cover increases ground reflection and thus increasing the electricity generation during the winter season. This increase was verified with the urban scenario not to be due exclusively to a different tilt angle, and really to be due the albedo of snow. Extended snow cover duration could be profitable for PV installations and reduce the power demand mismatch in winter.

Some further improvements could be suggested: to have a tighter pixel size for radiation data to match them with precise terrain data. These data, as elevation, slope, snow cover are available at high spatial resolution and are highly variable in a country like Switzerland. The slope of the terrain for the snow scenario should also be taken account, in order to avoid having to install

panels in a place with a high slope, and complicating thus the logistics. The snow data obtained form MODIS could be compared to in-situ measurements at IMIS[6] or BEOB[7] stations (observator stations form SLF), for example, to better interpolate the missing data. The other limitation, linked with snow, are the snowfalls that recover the panels and then make the energy generation impossible. In this case, either a solution to remove the snow quickly has to be found or take into account potential production losses due to snow recovering PV panels (Andrews 2013).

[6]http://www.slf.ch/schneeinfo/messwerte/stationsdaten/zeitverlauf_FR

[7]http://www.slf.ch/ueber/organisation/warnung_praevention/projekte/beobachter/index_FR

References

A. Riggs, G., D. K.Hall, and M. Roman (2016). "MODIS Snow Products Collection 6 User guide". In:

Andrews Pollard, Pearce (2013). "The effects of snowfall on solar photovoltaic performance". In: *Solar Energy* 92. URL: http://www.sciencedirect.com/science/article/pii/S0038092X13000790 (visited on 10/31/2016).

Bartlett, Stuart John et al. (2015). "Risks and Reliability in a Fully Renewable Switzerland". In: *European Safety and Reliability Conference 2015*. URL: http://infoscience.epfl.ch/record/208855 (visited on 01/09/2017).

doi:10.1016/j.rse.2006.06.009 - Stroeve et al RSE 2006.pdf (2016). URL: http://bprc.osu.edu/~jbox/pubs/Stroeve%20et%20al%20RSE%202006.pdf (visited on 07/14/2016).

Duffie, John A. and William A. Beckman (2013a). "Cover". In: *Solar Engineering of Thermal Processes, 4th Edition*. 4th ed. John Wiley & Sons. ISBN: 978-1-118-41541-2. URL: http://proquest.safaribooksonline.com/book/energy/9781118415412/firstchapter (visited on 01/09/2017).

— (2013b). "Introduction". In: *Solar Engineering of Thermal Processes, 4th Edition*. 4th ed. John Wiley & Sons. ISBN: 978-1-118-41541-2. URL: http://proquest.safaribooksonline.com/book/energy/9781118415412/firstchapter (visited on 01/09/2017).

Energiestrategie 2050 (2017). URL: http://www.bfe.admin.ch/energiestrategie2050/ (visited on 01/09/2017).

Gray, D. M. and P. G. Landine (1987). "Albedo model for shallow prairie snow covers". In: *Canadian Journal of Earth Sciences* 24.9, pp. 1760–1768. URL: http://www.nrcresearchpress.com/doi/abs/10.1139/e87-168 (visited on 10/22/2016).

He, Z. H. et al. (2014). "Estimating degree-day factors from MODIS for snowmelt runoff modeling". In: *Hydrology and Earth System Sciences* 18.12, pp. 4773–4789. ISSN: 1607-7938. DOI: 10.5194/hess-18-4773-2014. URL: http://www.hydrol-earth-syst-sci.net/18/4773/2014/ (visited on 05/03/2016).

Heintzenberg, J. and Robert J. Charlson, eds. (2009). *Clouds in the perturbed climate system: their relationship to energy balance, atmospheric dynamics, and precipitation*. Strüngmann Forum reports. OCLC: 262881413. Cambridge, Mass: MIT Press. 597 pp. ISBN: 978-0-262-01287-4.

Hüsler, F (2014). "A satellite-based snow cover climatology (1985-2011) for the European Alps derived from AVHRR data". In: *The Cryosphere* 8, pp. 73–90. URL: http://www.the-cryosphere.net/8/73/2014 (visited on 10/22/2016).

Klein, Andrew G. and J.C. Stroeve (2002). *Annals of Glaciology 34: 45-52 , Development and validation of a snow albedo algorithm for the MODIS instrument*. Cambridge CB2 1ER United Kingdom: International glaciology society.

Luna, D., J.-P. Nadeau, and Y. Jannot (2010). "Model and simulation of a solar kiln with energy storage". In: *Renewable Energy* 35.11, pp. 2533–2542. ISSN: 09601481. DOI: 10.1016/j.renene.2010.03.024. URL: http://linkinghub.elsevier.com/retrieve/pii/S0960148110001412 (visited on 10/22/2016).

Mehleri, E. D. et al. (2010). "Determination of the optimal tilt angle and orientation for solar photovoltaic arrays". In: *Renewable Energy* 35.11, pp. 2468–2475. ISSN: 0960-1481. DOI: 10.1016/j.renene.2010.03.006. URL: http://www.sciencedirect.com/science/article/pii/S0960148110001084 (visited on 10/22/2016).

MODIS Web (2016). URL: http://modis.gsfc.nasa.gov/about/design.php (visited on 06/07/2016).

Muis, Z.A. et al. (2010). "Optimal planning of renewable energy-integrated electricity generation schemes with CO2 reduction target". In: *Renewable Energy* 35.11, pp. 2562–2570. ISSN: 09601481. DOI: 10.1016/j.renene.2010.03.032. URL: http://linkinghub.elsevier.com/retrieve/pii/S0960148110001497 (visited on 10/22/2016).

Optimum Tilt of Solar Panels (2016). URL: http://solarpaneltilt.com/ (visited on 10/22/2016).

Plugin Grille pour QGIS - Manuel grille.pdf (2016). URL: https://orbi.ulg.ac.be/bitstream/2268/184045/1/Manuel%20grille.pdf (visited on 10/22/2016).

Rappaport, Fabrice. "Section Editors". In:

Ross, M. M. D. (1995). "Snow and ice accumulation on photovoltaic arrays: An assessment of the TN conseil passive melting technology, report# EDRL 95-68 (TR), energy diversification research laboratory, CANMET". In: *Natural Resources Canada, Varennes*. URL: http://www.rerinfo.ca/documents/trPVSnowandRime.pdf (visited on 10/31/2016).

Salazar, Germán A., Alejandro L. Hernández, and Luis R. Saravia (2010). "Practical models to estimate horizontal irradiance in clear sky conditions: Preliminary results". In: *Renewable Energy* 35.11, pp. 2452–2460. ISSN: 09601481. DOI: 10.1016/j.renene.2010.01.033. URL: http://linkinghub.elsevier.com/retrieve/pii/S0960148110000984 (visited on 10/22/2016).

Salomonson, V.V and I Appel (2004). "Estimating fractional snow cover from MODIS using the normalized difference snow index". In: *Remote Sensing of Environment* 89.3, pp. 351–360. ISSN: 00344257. DOI: 10.1016/j.rse.2003.10.016. URL: http://linkinghub.elsevier.com/retrieve/pii/S0034425703002864 (visited on 06/05/2016).

Stöckli, Reto (2013). "The HelioMont Surface Solar Radiation Processing". In: *Federal Office of Meteorology and Climatology,Scientific Report MeteoSwiss* 93.11.

Tang, Zhiguang et al. (2014). "Extraction and assessment of snowline altitude over the Tibetan plateau using MODIS fractional snow cover data (2001 to 2013)". In: *Journal of Applied Remote Sensing* 8.1, p. 084689. ISSN: 1931-3195. DOI: 10.1117/1.JRS.8.084689. URL: http://remotesensing.spiedigitallibrary.org/article.aspx?doi=10.1117/1.JRS.8.084689 (visited on 07/16/2016).

Townsend, Tim and Loren Powers (2011). "Photovoltaics and snow: An update from two winters of measurements in the SIERRA". In: IEEE, pp. 003231–003236. ISBN: 978-1-4244-9965-6 978-1-4244-9966-3 978-1-4244-9964-9. DOI: 10.1109/PVSC.2011.6186627. URL: http://ieeexplore.ieee.org/document/6186627/ (visited on 10/31/2016).

Vermeylen, Saskia (2010). "Resource rights and the evolution of renewable energy technologies". In: *Renewable Energy* 35.11, pp. 2399–2405. ISSN: 09601481. DOI: 10.1016/j.renene.2010.03.017. URL: http://linkinghub.elsevier.com/retrieve/pii/S0960148110001345 (visited on 10/22/2016).

Wang, Mo and Kamran Siddiqui (2010). "The impact of geometrical parameters on the thermal performance of a solar receiver of dish-type concentrated solar energy system". In: *Renewable Energy* 35.11, pp. 2501–2513. ISSN: 09601481. DOI: 10.1016/j.renene.2010.03.021. URL: http://linkinghub.elsevier.com/retrieve/pii/S0960148110001382 (visited on 10/22/2016).

www.sumointeractive.com (2017). *Energyscope*. Energyscope. URL: http://www.energyscope.ch/100-questions/energies-renouvelables/quel-est-le-potentiel-de-l-energie-solaire-en-suisse (visited on 01/09/2017).

Appendix

CORINE LAND COVER LEGEND

Level 1	Level 2	Level 3	Grid_Code	RGB
1. ARTIFICIAL SURFACES	1.1Urban fabric	1.1.1 Continuous urban fabric	1	230-000-077
		1.1.2 Discontinuous urban fabric	2	255-000-000
	1.2 Industrial, commercial and transport units	1.2.1 Industrial or commercial units	3	204-077-242
		1.2.2 Road and rail networks and associated land	4	204-000-000
		1.2.3 Port areas	5	230-204-204
		1.2.4 Airports	6	230-204-230
	1.3 Mine, dump and construction sites	1.3.1 Mineral extraction sites	7	166-000-204
		1.3.2 Dump sites	8	166-077-000
		1.3.3 Construction sites	9	255-077-255
	1.4 Artificial, non-agricultural vegetated areas	1.4.1 Green urban areas	10	255-166-255
		1.4.2 Sport and leisure facilities	11	255-230-255
2. AGRICULTURAL AREAS	2.1 Arable land	2.1.1 Non-irrigated arable land	12	255-255-168
		2.1.2 Permanently irrigated land	13	255-255-000
		2.1.3 Rice fields	14	230-230-000
	2.2 Permanent crops	2.2.1 Vineyards	15	230-128-000
		2.2.2 Fruit trees and berry plantations	16	242-166-077
		2.2.3 Olive groves	17	230-166-000
	2.3 Pastures	2.3.1 Pastures	18	230-230-077
	2.4 Heterogeneous agricultural areas	2.4.1 Annual crops associated with permanent crops	19	255-230-166
		2.4.2 Complex cultivation patterns	20	255-230-077
		2.4.3 Land principally occupied by agriculture, with significant areas of natural vegetation	21	230-204-077
		2.4.4 Agro-forestry areas	22	242-204-166
3. FOREST AND SEMI NATURAL AREAS	3.1Forests	3.1.1 Broad-leaved forest	23	128-255-000
		3.1.2 Coniferous forest	24	000-166-000
		3.1.3 Mixed forest	25	077-255-000
	3.2 Scrub and/or herbaceous vegetation associations	3.2.1 Natural grasslands	26	204-242-077
		3.2.2 Moors and heathland	27	166-255-128
		3.2.3 Sclerophyllous vegetation	28	166-230-077
		3.2.4 Transitional woodland-shrub	29	166-242-000
	3.3 Open spaces with little or no vegetation	3.3.1 Beaches, dunes, sands	30	230-230-230
		3.3.2 Bare rocks	31	204-204-204
		3.3.3 Sparsely vegetated areas	32	204-255-204
		3.3.4 Burnt areas	33	000-000-000
		3.3.5 Glaciers and perpetual snow	34	166-230-204
4. WETLANDS	4.1 Inland wetlands	4.1.1 Inland marshes	35	166-166-255
		4.1.2 Peat bogs	36	077-077-255
	4.2 Maritime wetlands	4.2.1 Salt marshes	37	204-204-255
		4.2.2 Salines	38	230-230-255
		4.2.3 Intertidal flats	39	166-166-230
5. WATER BODIES	5.1 Inland waters	5.1.1 Water courses	40	000-204-242
		5.1.2 Water bodies	41	128-242-230
	5.2 Marine waters	5.2.1 Coastal lagoons	42	000-255-166
		5.2.2 Estuaries	43	166-255-230
		5.2.3 Sea and ocean	44	230-242-255
No Data	No Data		48	
	No Data		49	
	No Data		50	230-242-255

List of Matalb codes used in the project :

- Compute_Ratio_Diffuse2Global.m

  Code provided by A.K : Computes the ratio for diffuse to global radiation with two relations: ERBS and Orgill Holland. (Duffie and Beckman, 2013).

- Compute_solar_angles.m

  Code provided by A.K: Computes the solar zenith angle and solar azimuth angle for each SIS pixel

- Radiation_onTiltedPanel_loop.m

  Code provided by A.K: "Computes the three components of solar radiation onto tilted panel surface"(Annelen Kahl). Total panel incoming shortwave = I beam + I ground reflected + I diffuse

- Transform_SISbeam2BeamParallel.m

  Code provided by A.K : transforms the beam part of SIS to beam parallel radiation

- MODIStoSIS.m

  Converts the tile obtained from MODIS to an SIS grid

- interpolation.m

  Interpolates the missing values of snow cover and albedo

- Corin_land_use.m

  Converts the corin shape file into an SIS grid and assignes a reflectance value to the corine's classes.

- Snow_duration.m computes the number of days covered with snow for each pixel

- scenario_urban_popdensity_AK.m

  Computes the needed panel surface with PV on rooftops

- scenario_snow_AK.m

  Computes the needed panel surface with PV in areas with high snow cover

- compare_urbanVSsnow.m

  Comapres both scenarios

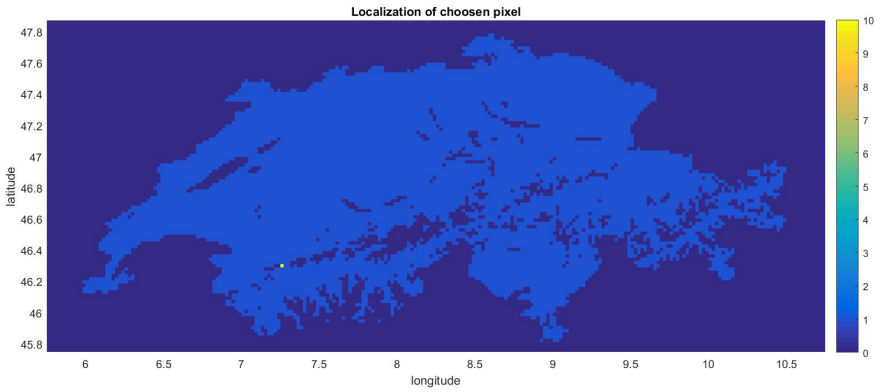

Figure 16: *Localization of chosen pixel, for fig.6, fig.7, fig 16, fig 17.*

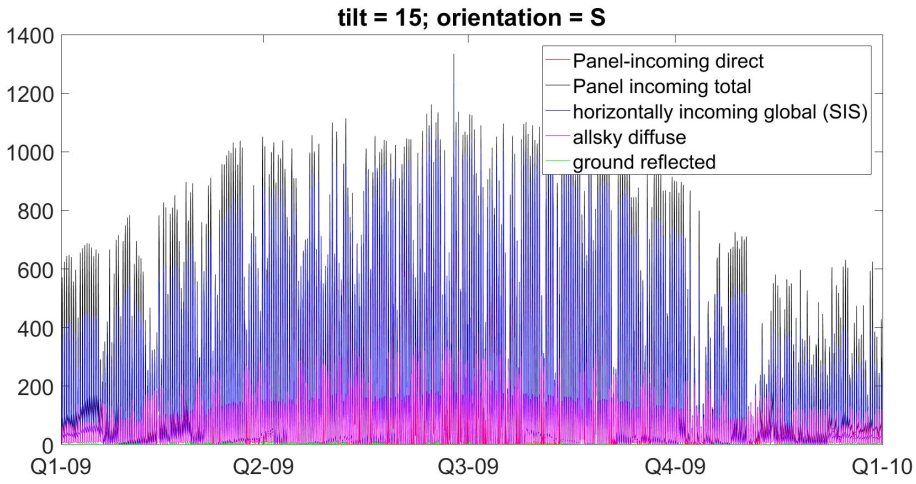

Figure 17: *Behaviour of PIS components with a tilt angle of 15°and a south orientation*

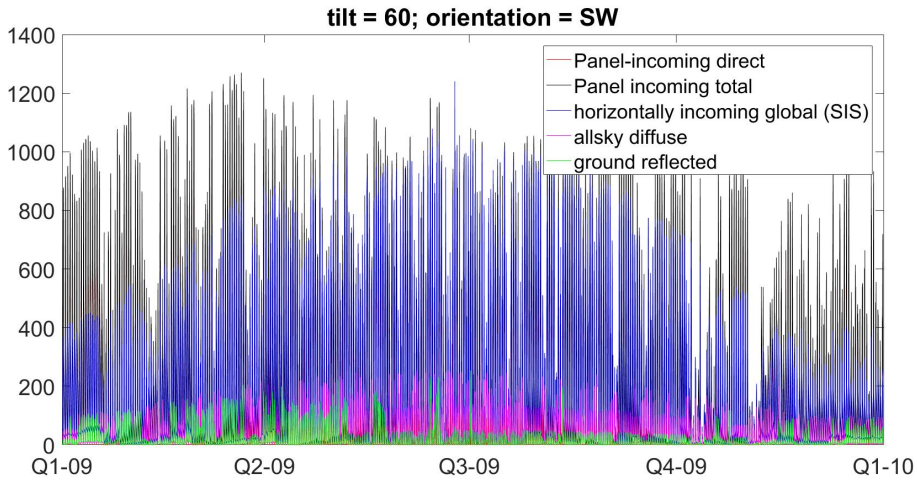

Figure 18: *Behaviour of PIS components with a tilt angle of 60°and a south-west orientation*

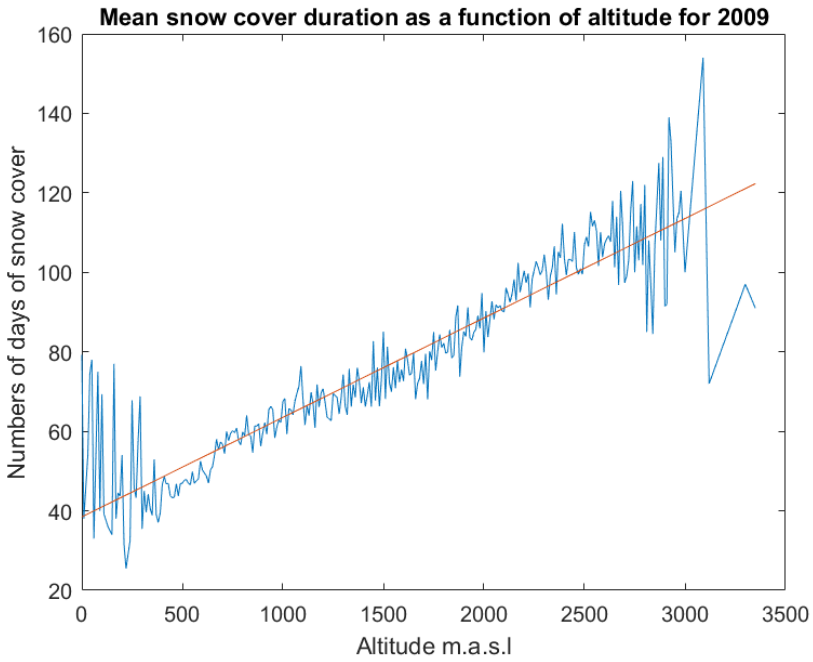

Figure 19: *2009*

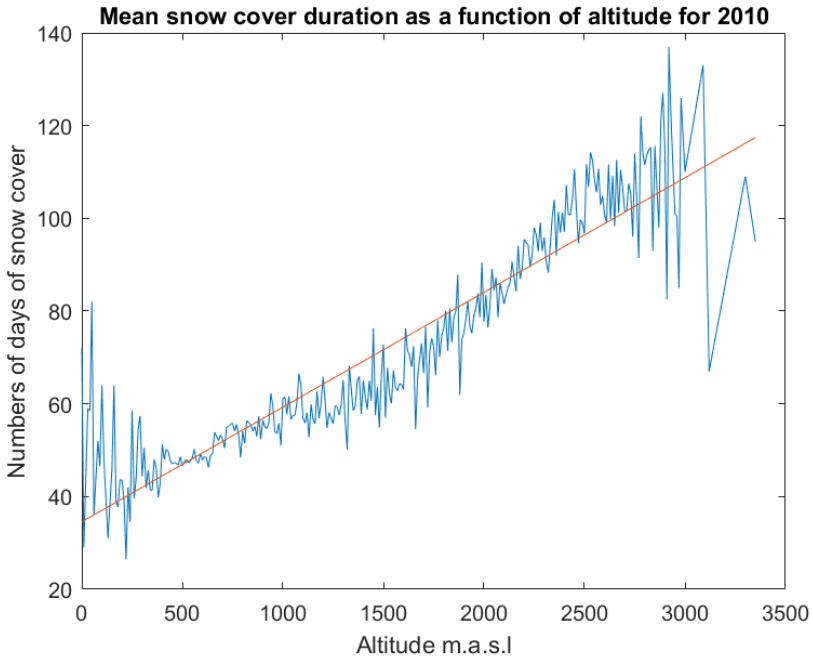

Figure 20: *2010*

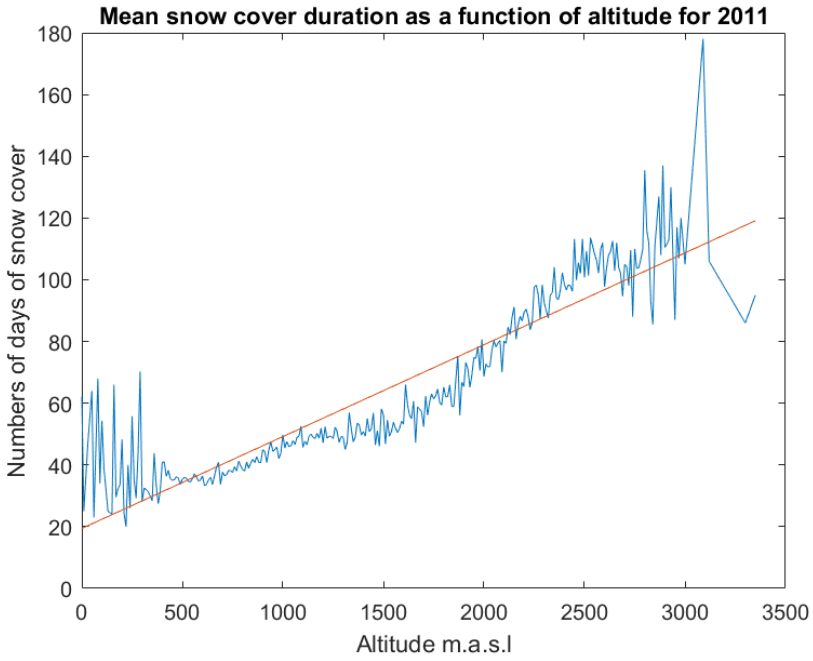

Figure 21: *2011*

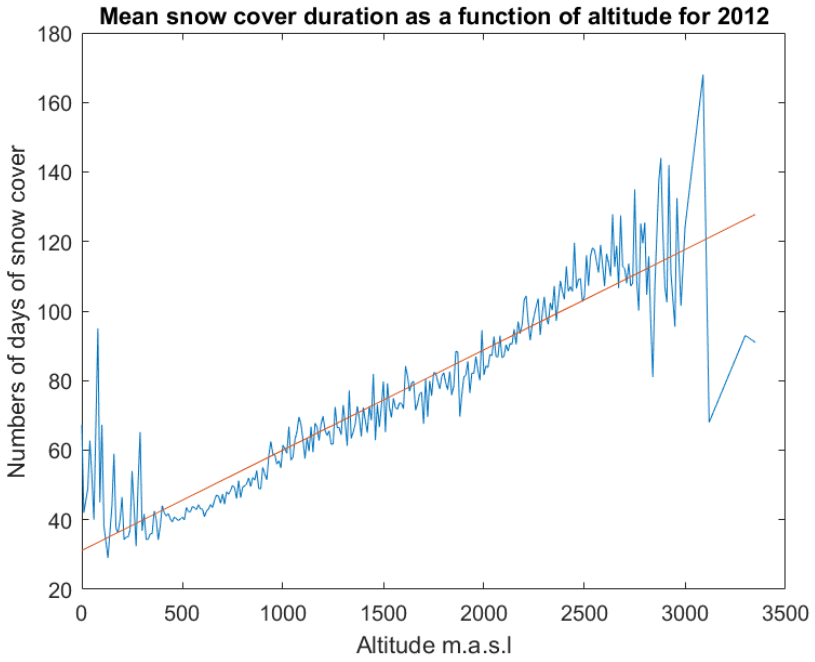

Figure 22: *2012*

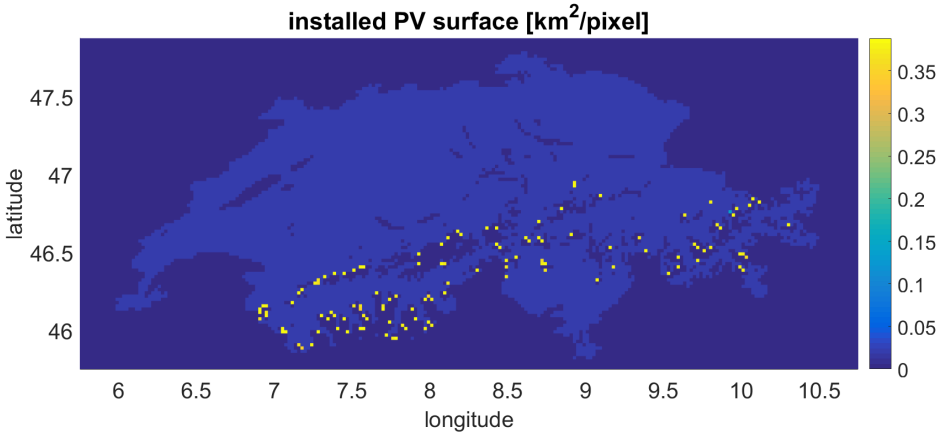

Figure 23: *Snow scenario for 2013*

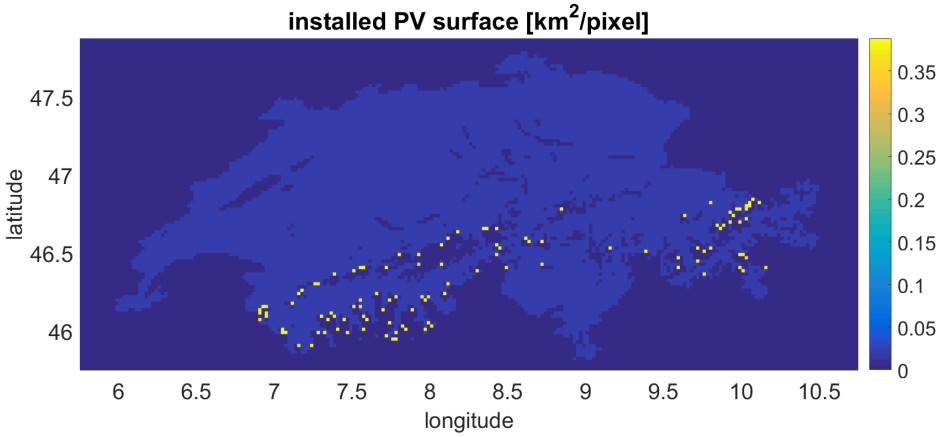

Figure 24: *Snow scenario for 2011*

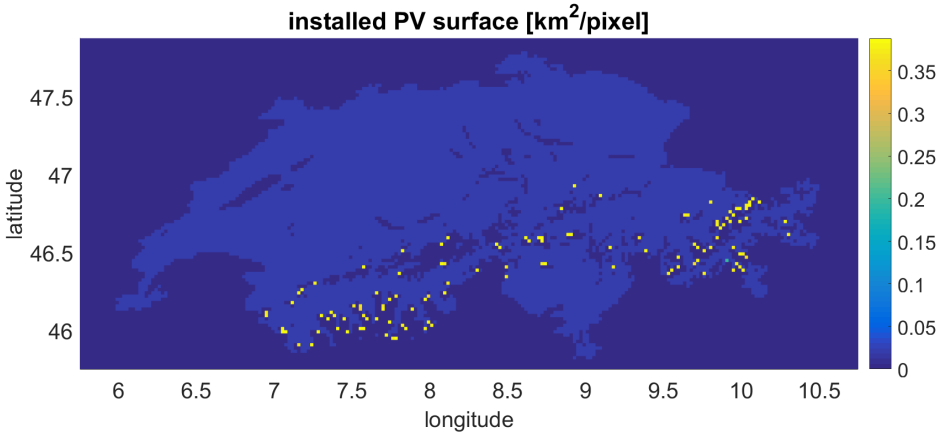

Figure 25: *Snow scenario for 2010*

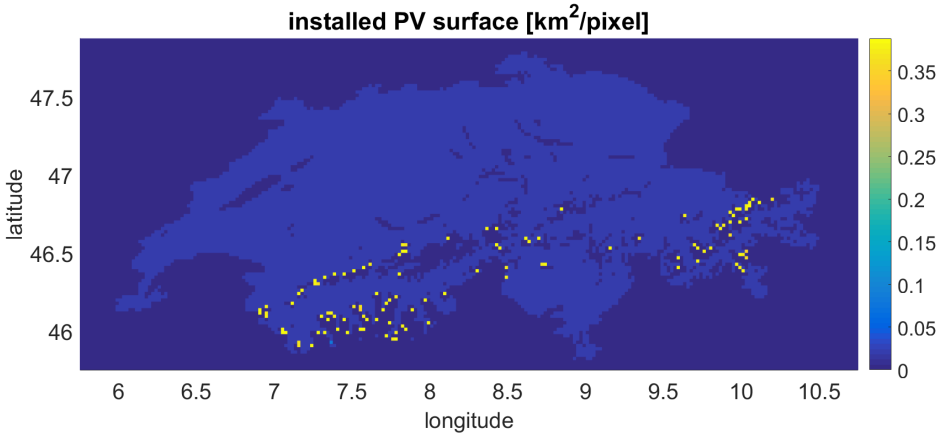

Figure 26: *Snow scenario for 2009*

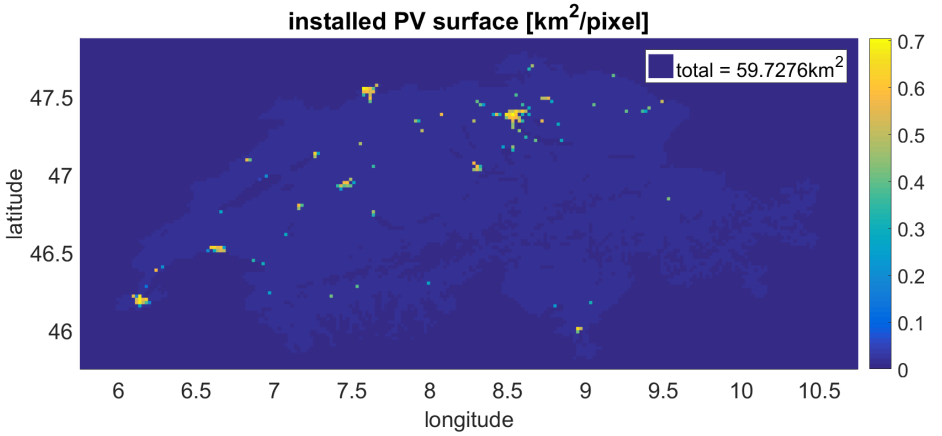

Figure 27: *Urabn scenario 2013*

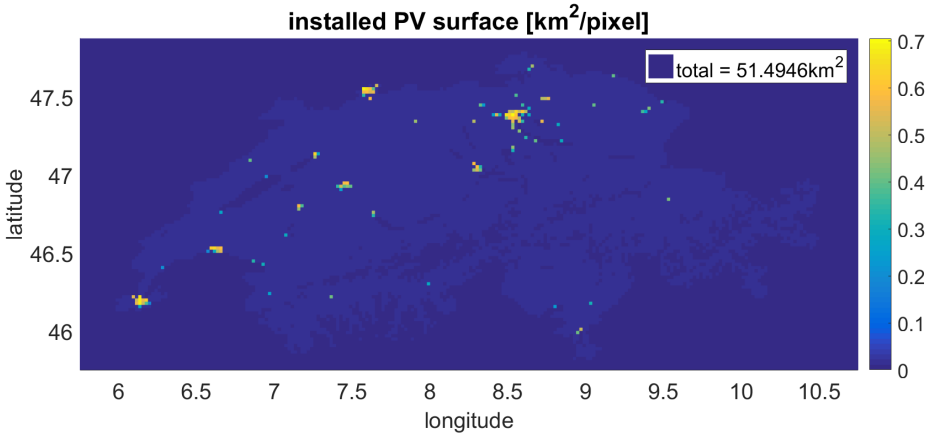

Figure 28: *Urabn scenario for 2011*

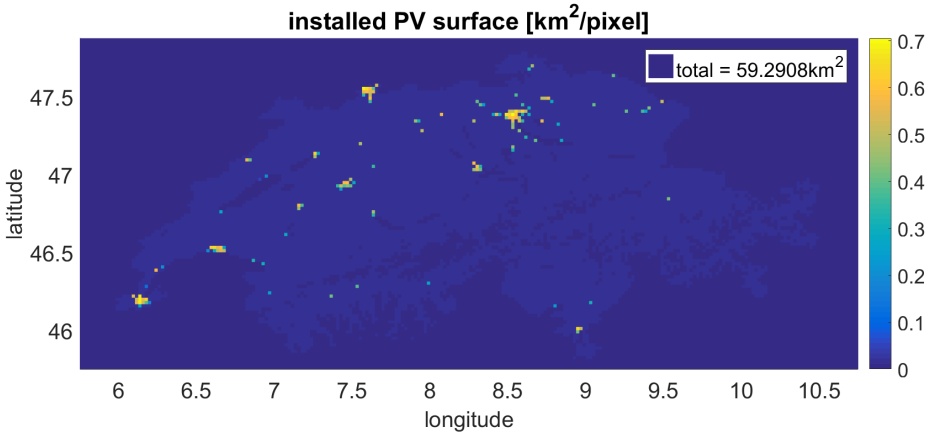

Figure 29: *Urabn scenario for 2010*

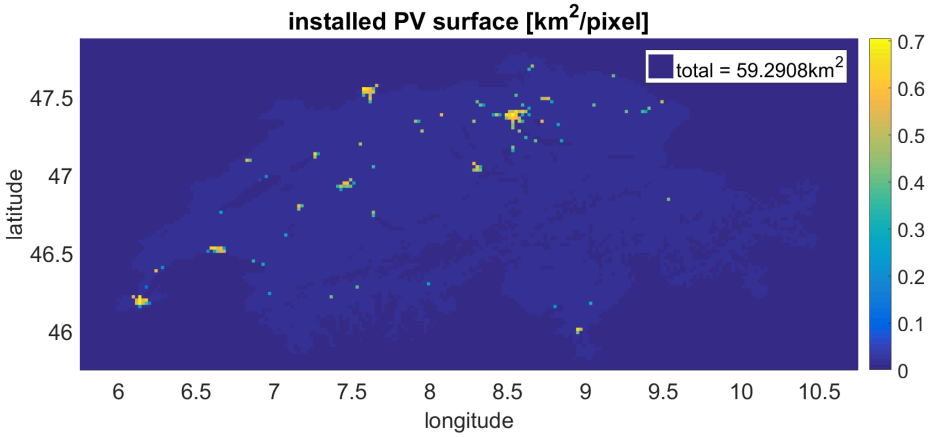

Figure 30: *Urabn scenario for 2009*